

8.5 DISPLACEMENT CASCADE SIMULATION IN TUNGSTEN UP TO 200 KEV OF DAMAGE

ENERGY AT 300, 1025, AND 2050 K — W. Setyawan, G. Nandipati, K. Roche, R. J. Kurtz (Pacific Northwest National Laboratory) and B. D. Wirth (University of Tennessee, Knoxville)

OBJECTIVE

The objective of this research is to support the prediction of irradiation damage properties of bulk tungsten-based materials using computational methods. In particular, to provide distributions of primary defects as inputs for kinetic Monte Carlo simulations of damage evolution and accumulation in tungsten.

SUMMARY

We generated a molecular dynamics database of primary defects that adequately covers the range of tungsten recoil energy imparted by 14-MeV neutrons. During this semi annual period, cascades at 150 and 200 keV at 300 and 1025 K were simulated. Overall, we included damage energy up to 200 keV at 300 and 1025 K, and up to 100 keV at 2050 K. We report the number of surviving Frenkel pairs (N_F) and the size distribution of defect clusters. The slope of the N_F curve versus cascade damage energy (E_{MD}), on a log-log scale, changes at a transition energy (μ). For $E_{MD} > \mu$, the cascade forms interconnected damage regions that facilitate the formation of large clusters of defects. At 300 K and $E_{MD} = 200$ keV, the largest size of interstitial cluster and vacancy cluster is 266 and 335, respectively. Similarly, at 1025 K and $E_{MD} = 200$ keV, the largest size of interstitial cluster and vacancy cluster is 296 and 338, respectively. At 2050 K, large interstitial clusters also routinely form, but practically no large vacancy clusters do.

PROGRESS AND STATUS

Simulation details

The molecular dynamics (MD) simulations were performed using LAMMPS software [1]. For the W-W interaction, the Finnis-Sinclair potential developed by Ackland and Thetford [2] was taken, in which the short-range part was then modified to harden the repulsion [3]. Modification was also done at distances relevant to self-interstitial configurations to improve defect formation energies. Before a displacement cascade was initiated, the system was thermalized in the NPT ensemble for 50 ps with a Nosé-Hoover thermostat to generate a canonical distribution of positions and velocities at the intended temperature. Subsequently, a primary-knock-on atom (PKA) was randomly chosen near the center of the simulation box and assigned an initial velocity with a random direction. Periodic boundaries were employed. The simulation was discarded if an atom crossed the boundaries. Electronic losses were not considered. Therefore, the PKA energy corresponds to the cascade damage energy (E_{MD}). The details of the simulations for cascades up to 100 keV can be found in [4]. Cascades at 150 and 200 keV at 300 and 1025 K were simulated using the following procedure. NVE ensemble was used throughout the cascade simulations, except for atoms within two lattice units of the boundaries (border atoms). A Nosé-Hoover thermostat with a time constant of 50 fs was applied to these border atoms to model the heat conduction out of the box. The simulations were followed up to 75 ps (default setting), or beyond 75 ps in a few cases, to ensure that the number of surviving Frenkel pairs (N_F) remained constant for at least 25 ps. Wigner-Seitz cell analysis was employed to detect the defects. Self-interstitial (SIA) clustering was searched with connectivity up to the third nearest-neighbor distance (NN3), while NN4 was used for detecting vacancy clusters, as suggested in [5].

Updated Results

The calculated melting temperature of the empirical potential is $T_m = 4100 \pm 50$ K [3], compared to the experimental value of 3695 K. The displacement threshold energy, averaged over all directions, was calculated to be $E_d = 122.6 \pm 4.4$ eV [4]. Table 1 summarizes the size of simulation box (L), the number of simulations (N_s), N_F , and the standard deviation (STD) of N_F for all damage energies that we have explored. In Table 1, the first horizontal line between 0.3 and 0.5 keV indicates the approximate energy above which $N_F > 1$. The second horizontal line between 30 and 40 keV for 300 and 1025 K, and between

20 and 30 keV for 2050 K, indicates the approximate energy in which the morphology of the cascade changes from single supersonic shock (SS) to interacting multiple supersonic shocks (iMS) [4].

Table 1. List of cascade damage energies (E_{MD}), simulation cells (cubes with side length L), number of simulations (N_r), and number of surviving Frenkel pairs (N_F) with the standard deviation (STD). The lattice constants (a) at 300, 1025, and 2050 K are 3.167, 3.184, and 3.216 Å, respectively. The displacement threshold energy, averaged over all directions, is $E_d = 122.6$ eV.

E_{MD} (keV)	E_{MD}/E_d	L (a)	300 K			1025 K			2050 K		
			N_r	N_F	STD	N_r	N_F	STD	N_r	N_F	STD
0.1	0.82	15	40	0.45	0.5	40	0.30	0.5	40	0.45	0.5
0.15	1.22	15	40	0.55	0.5	40	0.33	0.5	40	0.45	0.5
0.2	1.63	15	40	0.58	0.5	40	0.38	0.5	40	0.60	0.5
0.3	2.45	15	40	0.85	0.6	40	0.80	0.6	40	0.63	0.6
0.5	4.08	20	20	1.4	0.7	20	1.3	0.6	20	1.1	0.7
0.75	6.12	20	20	1.8	1.0	20	1.4	1.1	20	1.6	0.9
1	8.16	30	20	2.2	1.0	20	1.8	0.8	20	1.7	1.3
1.5	12.2	30	20	3.1	1.2	20	2.4	1.6	20	2.4	0.8
2	16.3	30	20	3.9	1.7	20	2.6	1.5	20	2.7	1.3
3	24.5	30	20	4.7	1.8	20	4.4	1.5	20	3.5	2.0
5	40.8	40	20	7.1	2.3	20	5.2	2.0	20	5.8	2.1
7.5	61.2	40	20	9.7	3.3	20	7.0	2.2	20	5.8	2.0
10	81.6	50	20	12.0	2.8	15	9.3	2.5	15	9.3	1.3
15	122.4	50	20	15.0	3.5	15	13.6	3.7	15	10.9	3.0
20	163.1	64	20	21.2	5.1	15	18.0	3.5	15	15.1	5.0
30	244.7	64	20	27.2	5.5	15	22.4	6.0	15	21.7	5.9
40	326.3	64	15	34.7	7.0	15	31.7	7.4	15	32.5	4.9
50	407.8	80	15	49.9	11.0	15	43.2	9.7	15	39.3	8.4
60	489.4	80	15	60.9	20.8	15	52.9	12.0	15	53.4	17.7
75	611.8	100	15	81.5	20.4	15	80.9	29.9	15	77.1	28.9
100	815.7	120	20	116	35.3	20	111	29.3	20	107	29.5
150	1223	160	10	226	109	-	-	-	-	-	-
150	1223	180	-	-	-	10	200	91.3	-	-	-
200	1631	180	10	315	81	-	-	-	-	-	-
200	1631	200	-	-	-	10	320	131	-	-	-

Figure 1 shows the updated plots of N_F versus E_{MD} . The data points are fitted with a bilinear curve by using a linear-least-square minimization on a log-log scale. The resulting empirical formulas of N_F as a function of E_{MD} are shown in Figure 1. The kink in the bilinear fit is defined as the transition energy (μ) corresponding to a SS \rightarrow iMS morphological transition. The transition occurs at 37, 31, and 25 keV for cascades at 300, 1025, and 2050 K, respectively. The new cascade data at 150 and 200 keV follow the trend of the data above μ . Future studies may include higher energies to explore the possibility that another transition of cascade morphology might occur.

Clustering data of the defects are summarized in Table 2Table 4. Evidently, large clusters of size 30 or more, and even of size 200 or more, form for $E_{MD} > \mu$. The defect distribution for $E_{MD} > \mu$ is significantly different from that for $E_{MD} < \mu$. Therefore, properly including primary defects from cascades below and above the transition energy is suggested in kinetic Monte Carlo simulations of damage accumulation in tungsten.

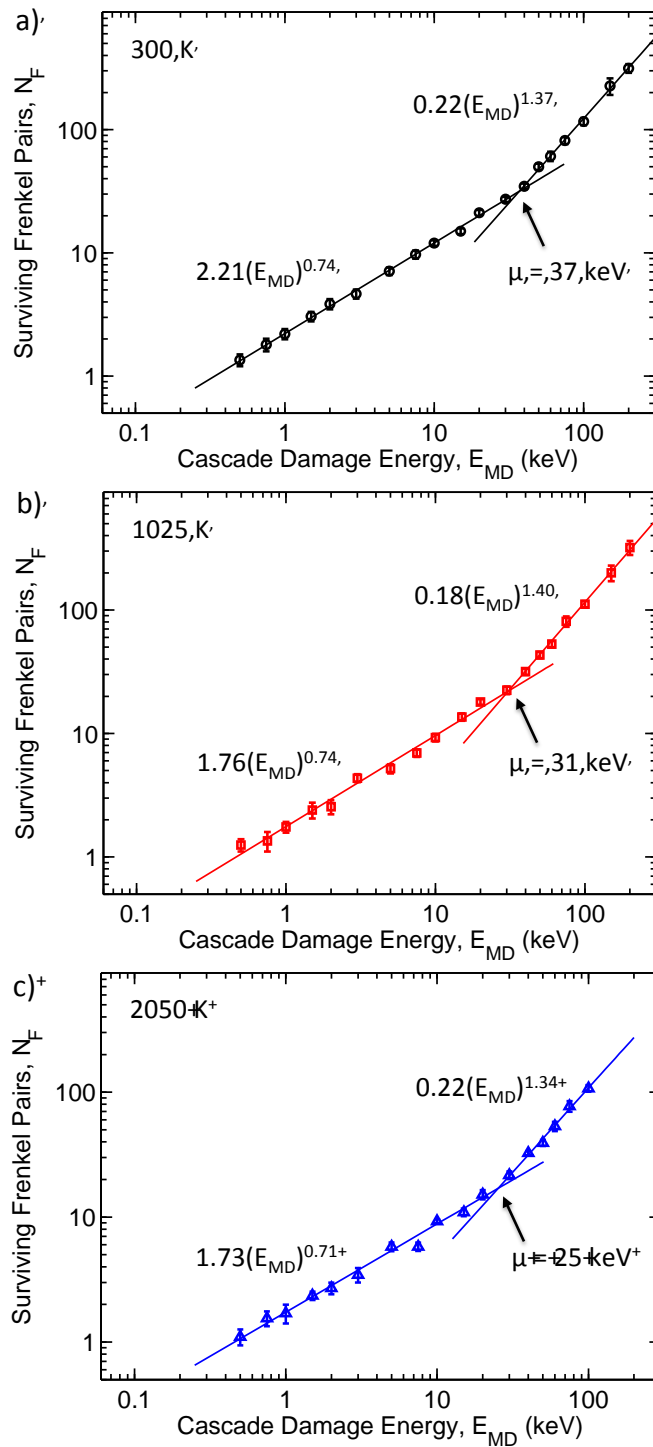


Figure 1. Number of surviving Frenkel pairs as a function of cascade damage energy. A bilinear curve is employed to fit the data. The kink in the curve is defined as the transition energy (μ).

Table 2. Counting data of SIA clusters (top panel) with connectivity up to NN3 and vacancy clusters (bottom panel) up to NN4 at 300 K. E_{MD} denotes the cascade damage energy. N_r denotes the number of simulations.

E_{MD} (keV)	N_r	Number of clusters (C_j) listed in order, starting from cluster of size $S_j = 1, 2, 3 \dots$, or given in C_j/S_j format.
1	20	38 3 0 0 0
1.5	20	48 5 1 0 0
2	20	58 5 3 0 0
3	20	54 8 2 3 1
5	20	102 12 2 1 0 1/6
7.5	20	114 14 7 5 1 1/6
10	20	137 29 4 1 4 0 1 0 0 0
15	20	158 31 8 7 3 1 1 0 0 0
20	20	220 31 10 6 3 2 2 1 1 0 1/12 1/16
30	20	263 38 9 7 3 2 5 1 1 2 1/11 1/12 1/13 1/14
40	15	255 35 15 7 2 1 1 3 0 1 2 1 0 0 1 1/16
50	15	276 34 7 7 7 3 0 3 4 1 0 0 2 0 1 1/18 1/21 2/23 2/24 1/27 1/32
60	15	326 50 8 6 5 5 2 3 2 0 1 1 1 0 0 1 0 0 0 0 1/21 1/22 1/23 1/25 1/27 1/31 1/36 1/41 1/50
75	15	391 60 20 7 7 8 6 2 1 5 2 1 0 0 1 0 0 1 0 1 1/24 1/26 1/27 1/37 2/38 1/45 1/46 1/56
100	20	666 74 27 18 10 11 3 3 4 3 4 2 1 1 2 2 2 1 0 2 1 1 3 0 0 0 1 1 0 2 1/33 1/38 1/40 1/41 1/57 2/61 2/63 2/65 1/70
150	10	408 65 19 11 10 5 5 3 3 1 1 1 1 2 1 1 0 1 0 1 1 0 0 0 1 0 1 1 2 2 1/31 1/39 1/40 1/45 1/50 1/71 1/72 1/83 1/91 1/97 1/110 1/115 1/250
200	10	513 55 33 13 7 7 4 2 4 2 3 1 1 0 0 1 2 3 1 0 1 1 0 0 0 1 0 0 2 1 1/31 1/35 1/36 1/38 1/39 1/48 1/51 1/56 1/61 1/64 1/65 1/70 1/72 1/76 1/83 1/87 1/138 2/170 1/195 1/266
1	20	16 6 4 1 0
1.5	20	22 6 5 3 0
2	20	32 7 4 1 0 1/7 1/8
3	20	41 6 4 3 2 1/6
5	20	55 12 4 4 3 2/6 1/8
7.5	20	80 16 11 1 3 3/6 1/12
10	20	95 16 11 3 3 5 2 0 1 0
15	20	138 25 3 8 3 2 3 0 0 0 1/11 1/12
20	20	188 33 21 5 5 1 3 0 0 2 1/14
30	20	254 54 15 7 3 1 4 2 1 0 1/16 1/19
40	15	273 46 13 8 4 1 0 2 0 1 0 1 0 0 0 1/20
50	15	267 50 13 6 6 2 3 3 2 3 0 0 0 1 0 1/18 1/22 1/29 1/30 1/34 1/37
60	15	348 50 19 7 6 1 0 1 2 1 0 0 1 2 0 0 0 0 0 0 1/29 1/43 1/51 1/70 1/74
75	15	449 75 24 11 5 2 2 1 0 1 1 4 0 0 0 1 1 0 0 0 1/21 1/27 1/34 1/35 1/38 1/51 1/57 1/84
100	20	706 120 40 23 10 6 4 2 3 3 2 1 3 1 0 2 0 0 1 0 1 0 0 1 0 0 0 0 0 1/60 1/86 1/87 1/91 1/104 1/105 1/114 1/153
150	10	596 84 33 13 9 7 3 2 0 2 0 0 1 0 0 1 0 1 0 0 0 0 0 0 1 0 0 0 0 1/51 1/66 1/111 1/140 1/172 1/193 1/397
200	10	720 146 38 18 13 10 2 2 3 0 0 2 0 0 1 0 0 0 1 0 0 1 0 0 0 1 0 0 0 0 1/32 1/39 3/41 1/92 1/122 1/127 1/130 1/142 1/163 1/167 1/188 1/335

Table 3. Counting data of SIA clusters (top panel) with connectivity up to NN3 and vacancy clusters (bottom panel) up to NN4 at 1025 K. E_{MD} denotes the cascade damage energy. N_r denotes the number of simulations.

E_{MD} (keV)	N_r	Number of clusters (C_j) listed in order, starting from cluster of size $S_j = 1, 2, 3 \dots$, or given in C_j/S_j format.
1	20	28 2 1 0 0
1.5	20	39 2 0 0 1
2	20	44 2 1 0 0
3	20	62 5 2 1 1
5	20	80 7 1 0 0 1/7
7.5	20	90 10 5 1 2
10	15	100 14 1 2 0 0 0 0 0
15	15	115 13 4 2 1 2 0 2 0 1
20	15	143 22 5 2 1 4 3 0 0 1
30	15	148 21 9 4 7 2 2 1 0 1 1/11 1/13
40	15	186 23 15 6 1 6 1 1 1 0 1 0 0 1 1 1/20 1/22 1/26
50	15	228 40 9 4 3 3 0 2 2 2 0 1 1 1 0 1/20 2/22 1/31 1/35 1/41
60	15	240 40 9 3 1 4 0 3 2 2 1 2 0 0 0 1 1 1 0 3 2/22 1/24 2/27 1/28 1/47
75	15	292 47 15 8 4 4 1 2 4 1 4 0 1 0 2 2 0 0 1 1 1/23 2/25 1/26 1/27 1/47 1/51 1/56 1/57 1/68 1/75
100	20	513 76 28 13 3 2 9 3 1 2 2 5 2 1 6 1 1 2 1 0 0 4 0 1 1 2 1 0 1 0 2/32 1/37 1/41 1/44 1/52 1/54 1/59 1/71 1/72 1/73 1/77 1/97
150	10	313 60 11 9 3 6 3 4 3 2 0 0 2 1 4 0 2 1 0 0 1 1 0 0 1 0 0 0 0 1 2/31 1/34 2/43 1/48 1/53 1/56 1/57 1/67 1/76 1/77 1/79 1/97 1/104 1/201
200	10	384 69 31 11 2 7 3 2 2 2 1 4 4 1 1 2 1 2 0 1 1 1 2 1 0 0 1 0 1 0 2/31 1/32 1/33 1/37 1/40 1/44 1/45 1/52 1/58 1/59 1/67 1/69 2/75 1/90 1/91 1/106 1/124 1/128 1/155 1/267 1/296
1	20	12 10 1 0 0
1.5	20	20 8 2 0 0 1/6
2	20	20 10 1 2 0
3	20	46 7 3 3 0 1/6
5	20	53 12 3 2 2
7.5	20	72 20 3 2 2
10	15	83 20 4 1 0 0 0 0 0
15	15	96 31 8 1 1 1 1 0 0 0
20	15	137 31 7 1 5 1 1 1 0 0
30	15	177 43 7 7 2 1 0 1 0 0
40	15	268 41 4 7 1 1 1 0 2 1 0 1 1 1 0
50	15	300 45 17 6 2 2 4 2 1 2 1 0 1 0 0 1/18 1/21 1/25
60	15	407 66 20 7 5 3 2 4 2 0 0 0 0 0 0 0 0 0 1 0 1/41
75	15	451 88 21 8 4 0 3 0 4 0 0 1 0 1 2 0 2 0 0 0 1/21 1/46 1/56 1/82 1/120
100	20	838 141 34 15 13 2 1 5 3 0 1 0 0 1 1 0 0 0 1 1 1 0 0 0 1 1 0 1 0 0 1/42 1/58 1/73 1/74 2/83 1/88 1/117
150	10	650 90 25 13 3 5 3 1 4 0 0 1 1 0 0 0 0 0 1 0 0 0 0 0 0 0 0 0 0 0 1/32 1/35 1/36 1/42 1/124 1/160 1/197 1/263
200	10	892 153 38 29 11 5 4 2 1 2 3 2 1 0 0 0 0 0 1 0 1 0 0 0 1 1 1 0 0 0 1/38 1/39 1/57 1/77 1/90 1/132 1/165 1/169 1/326 1/338

Table 4. Counting data of SIA clusters (top panel) with connectivity up to NN3 and vacancy clusters (bottom panel) up to NN4 at 2050 K. E_{MD} denotes the cascade damage energy. N_r denotes the number of simulations.

E_{MD} (keV)	N_r	Number of clusters (C_j) listed in order, starting from cluster of size $S_j = 1, 2, 3 \dots$, or given in C_j/S_j format.
1	20	30 2 0 0 0
1.5	20	30 7 1 0 0
2	20	48 3 0 0 0
3	20	44 8 1 0 0 1/6
5	20	82 11 4 0 0
7.5	20	83 7 5 1 0
10	15	56 10 2 3 1 3 2 1 0 0
15	15	65 16 4 2 1 2 1 1 0 0 1/15
20	15	90 18 3 1 2 4 3 0 1 0 1/11 1/13
30	15	124 11 6 4 2 2 1 1 2 0 1/12 3/13 1/15 1/24
40	15	154 20 9 6 3 4 2 2 1 1 3 3 1 0 2 1/16 1/27
50	15	140 21 6 5 3 1 0 0 0 1 1 1 0 1 0 1/17 3/19 1/20 2/21 2/30 1/32 1/36 1/37
60	15	184 24 11 2 3 5 3 0 0 1 2 0 0 1 0 2 1 0 0 0 1/22 1/23 1/24 1/29 1/31 1/42 1/47 1/69 1/80
75	15	137 23 6 1 1 2 1 1 0 0 0 1 1 1 0 1 1 1 0 2 1/24 1/26 1/27 1/29 2/31 1/36 1/41 1/47 1/56 2/58 1/64 1/75 1/79 1/108
100	20	301 46 11 5 6 2 2 4 0 1 1 0 1 3 4 3 0 1 2 1 2 1 0 0 1 2 0 1 1 1 1/31 3/32 1/35 1/36 1/43 2/44 1/53 1/54 2/59 1/63 1/66 1/71 1/72 1/81 1/92 1/126
1	20	22 4 0 1 0
1.5	20	34 5 1 0 0
2	20	37 7 1 0 0
3	20	43 7 1 1 1
5	20	68 14 4 2 0
7.5	20	88 8 4 0 0
10	15	94 7 7 1 0 1 0 0 0 0
15	15	137 9 3 0 0 0 0 0 0 0
20	15	169 20 2 3 0 0 0 0 0 0
30	15	249 29 4 0 0 1 0 0 0 0
40	15	359 37 7 4 2 0 0 1 0 0 0 0 0 0
50	15	441 46 15 3 0 0 0 0 0 0 0 0 0 0
60	15	558 68 15 3 2 2 1 1 0 0 0 0 1 0 0 0 0 0 0
75	15	706 99 14 11 5 2 1 0 1 1 0 0 0 0 0 0 1 0 0 0 1/27 1/60
100	20	1339 146 35 16 11 6 3 0 1 4 2 0 0 2 1 0 0 0 0 0 0 1 0 0 0 0 0 0 0 1/38 1/60

References

- [1] S. Plimpton, J. Comp. Phys. 117 (1995) 1.
- [2] G.J. Ackland and T. Thetford, Phil. Mag. A 56 (1987) 15.
- [3] N. Juslin and B.D. Wirth, J. of Nuc. Mat. 432 (2013) 61.
- [4] W. Setyawan, A.P. Selby, N. Juslin, R.E. Stoller, B.D. Wirth and R.J. Kurtz, J. Phys: Cond. Matt. 27 (2015) 225402.
- [5] W. Setyawan, G. Nandipati, K.J. Roche, H.L. Heinisch, B.D. Wirth and R.J. Kurtz, J. Nuc. Mat. 462 (2015) 329.